Eur Biophys J (2007) 36:637–646
DOI 10.1007/s00249-007-0136-4

ORIGINAL PAPER

An investigation of the dynamics of spermine bound to duplex and quadruplex DNA by ^{13}C NMR spectroscopy

Max A. Keniry · Elisabeth A. Owen

Received: 18 October 2006 / Revised: 14 January 2007 / Accepted: 17 January 2007 / Published online: 15 February 2007

Abstract A detailed analysis of the ^{13}C relaxation of ^{13}C-labelled spermine bound to duplex and quadruplex DNA is presented. T_1, T_2 and heteronuclear NOE data were collected at four ^{13}C frequencies (75.4, 125.7, 150.9 and 201.2 MHz). The data were analyzed in terms of a frequency-dependent order parameter, $S^2(\omega)$, to estimate the generalized order parameter and the contributions to the relaxation from different motional frequencies in the picosecond–nanosecond timescale and from any exchange processes that may be occurring on the microsecond–millisecond timescale. The relaxation data was surprisingly similar for spermine bound to two different duplexes and a linear parallel quadruplex. Analysis of the relaxation data from these complexes confirmed the conclusions of previous studies that the dominant motion of spermine is independent of the macroscopic tumbling of the DNA and has an effective correlation time of ~50 ps. In contrast, spermine bound to a folded antiparallel quadruplex had faster relaxation rates, especially R_2. As with the other complexes, a fast internal motion of the order of 50 ps makes a substantial contribution to the relaxation. The generalized order parameter for spermine bound to duplex DNA and the linear quadruplex is small but is larger for spermine bound to the folded quadruplex. In the latter case, there is evidence for exchange between at least two populations of spermine occurring on the microsecond–millisecond timescale.

Keywords DNA · NMR spectroscopy · Spin relaxation · Order parameter · Nucleic acids · Spermine · Quadruplex

Introduction

The natural polyamines, spermine, spermidine and putrescine, are highly charged aliphatic cations that have essential roles in cell differentiation, proliferation, DNA synthesis and apoptosis (reviewed in Thomas and Thomas 2001). Although they are present in millimolar concentrations in all living cells (Tabor and Tabor 1984), the importance of polyamines to cellular function is reflected in the strict regulatory control of their intracellular concentration (Tabor and Tabor 1984). In general, polyamine concentrations are higher in cancer cells than normal cells and combined with their absolute requirement for growth and differentiation, polyamine metabolism and function has been linked to the initiation and progression of cancer (Marton and Pegg 1995).

The interaction of polyamines with nucleic acids is pivotal to their role in cellular processes yet they exert their influence mostly through weak interactions. Despite an extensive effort to determine and understand the molecular basis of this interaction, the location and dynamics of binding to nucleic acids is inadequately understood. There has been considerable debate over the specificity of the interaction with DNA and the influence of polyamines over the structure of DNA

Electronic supplementary material The online version of this article (doi:10.1007/s00249-007-0136-4) contains supplementary material, which is available to authorized users.

M. A. Keniry (✉) · E. A. Owen
Research School of Chemistry,
Australian National University,
Canberra, ACT 0200, Australia
e-mail: max@rsc.anu.edu.au

(Korolev et al. 2001, 2002). To date, no X-ray crystallographic or NMR study of the interaction of spermine with DNA has unequivocally located a specific interaction between spermine and B-DNA. In the crystallographic studies of several forms of DNA including A- and Z-DNA, the polyamines have been found in a variety of locations but most frequently near the phosphate backbone (Ohishi et al. 1996; Tippin and Sundaralingam 1997; Egli et al. 1998; Bancroft et al. 1994; Jain et al. 1989; Wang et al. 1979). Various other methods have placed spermine, either in the major groove (Ouameur and Tajmir-Riahi 2004; Ruiz-Chica et al. 2001) or the minor groove (Liquori et al. 1967; Schmid and Behr 1991). There is abundant evidence that spermine can alter the structure of DNA (e.g. converting some B-DNA sequences to the A- or the Z-conformation) but there is considerable debate about whether the binding preference is determined by direct readout of the sequence or by recognition of the secondary structure of the DNA (Ouameur and Tajmir-Riahi 2004). It is generally agreed that the driving force of DNA-nucleic acid association is electrostatic in origin and that hydrophobic interactions involving the methylene chains make a minor contribution (Thomas and Thomas 2001).

Much polyamine research has focused on the association with double-stranded DNA. There has been some work on spermine association with triple helices (Thomas and Thomas 1993) but little is known about whether spermine can distinguish between other structures such as loops or quadruplexes. We showed for the first time that spermine can bind to DNA quadruplexes and also discriminate between folded antiparallel quadruplexes and a linear parallel quadruplex (Keniry 2003). This is significant because DNA quadruplexes have been shown to act as transcriptional regulators (Hurley 2001; Siddiqui-Jain et al. 2002; Sun et al. 2005; Dai et al. 2006) and polyamines are known to alter the expression of genes associated with regulation, proliferation, differentiation and apoptosis (Berchtold et al. 1998).

The dynamic nature of the interaction of spermine with nucleic acids is just as interesting and important as its structural recognition properties. There are several lines of evidence for substantial spermine mobility on all forms of DNA. Spermine is rarely observed in crystals of B-DNA, although it is used to induce crystal formation. This implies a certain degree of mobility or delocalization. The most convincing evidence for the mobile nature of spermine on DNA comes from NMR studies (Andreasson et al. 1996; Wemmer et al. 1985; Banville et al. 1991; Van Dam and Nordenskiöld 1999). The observation of positive intramolecular ^{1}H–^{1}H NOEs between spermine protons and no intermolecular ^{1}H–^{1}H NOEs to the DNA protons prompted (Wemmer et al. 1985) to postulate that spermine had motion that was effectively independent of the rotational tumbling of B-DNA (Wemmer et al. 1985). They further proposed that spermine might diffuse along the DNA between tight binding sites (Wemmer et al. 1985). Subsequently, negative intramolecular NOEs were observed when spermine was bound to Z-DNA indicating that the spermine dynamics were slowed compared to spermine bound to B-DNA. We observed similar behaviour with some spermine-quadruplex complexes (Keniry 2003). The spermine had particularly strong negative intramolecular NOEs on binding to two different folded antiparallel quadruplexes but no intermolecular NOEs were observed (Keniry 2003). All of the NMR studies with various B-, Z- and quadruplex DNA structures have demonstrated an association with spermine but failed to unequivocally locate a specific interaction site (Van Dam and Nordenskiöld 1999; Wemmer et al. 1985; Banville et al. 1991).

All of this previous work presents only a qualitative picture of spermine dynamics providing only estimates of the effective correlation time of spermine reorientation on the DNA surface. In this present work, we have used the magnetic field dependence of ^{13}C nuclear relaxation to further elucidate the dynamics of spermine bound to DNA. We have measured, at four different magnetic field strengths, T_1, T_2 and the heteronuclear $\{^{1}H\}^{13}C$ NOE of ^{13}C-labelled spermine (Fig. 1a) bound to various DNA structures (Fig. 1b). These complexes include two B-conformation DNA duplexes and two quadruplexes. One duplex is a short self-complementary hexamer, $[d(ATGCAT)]_2$ and the other a complementary 13 mer that contains the recognition site of the dnaA initiation protein, $d(C_2TGTG_2ATA_2CA).d(TGT_2ATC_2ACAG_2)$ (Gray et al. 1994). The quadruplexes are a linear four-stranded DNA quadruplex $[d(TG_4T)]_4$, (Aboul-ela et al. 1992; Phillips et al. 1997) and a two-stranded diagonally looped folded quadruplex $[d(G_4T_4G_4)]_2$, (Smith and Feigon 1992). We used a Monte Carlo minimization procedure to calculate the frequency dependence of the order parameter for the $\alpha_{2''}$ carbon of spermine bound to each of the above structural forms of DNA. Using this approach, we have compared the contribution to the ^{13}C relaxation from the internal rotations, the overall tumbling of the DNA fragment and exchange processes. The findings build on our understanding of spermine dynamics provided by earlier studies that used only ^{1}H–^{1}H NOEs of DNA-bound spermine as a probe (Van Dam and Nordenskiöld 1999; Wemmer et al. 1985; Banville et al. 1991; Keniry 2003).

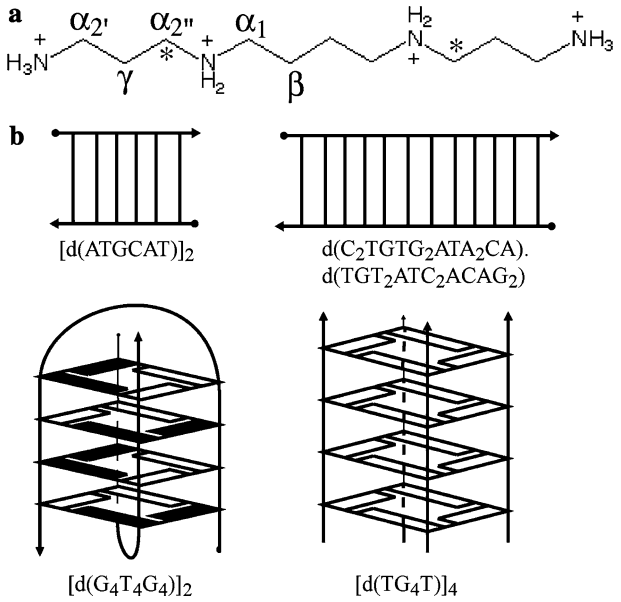

Fig. 1 **a** Diagrammatic representation of [1,1′-$^{13}C_2$]-spermine. The *asterisks* indicate the location of the ^{13}C label. **b** Diagrammatic representation of the oligonucleotide structures to which spermine is bound. $d(ATGCAT)_2$ and $d(C_2TGTG_2ATA_2CA).d(TGT_2ATC_2ACAG_2)$ are duplex B-DNA, $d(G_4T_4G_4)_2$ is a folded antiparallel two-stranded DNA quadruplex and $d(TG_4T)_4$ is a linear parallel four-stranded DNA quadruplex

Materials and methods

[1,1′-$^{13}C_2$]-^{13}C-Spermine synthesis and [1,1′-$^{13}C_2$]-spermine-DNA complex formation

[1,1′-$^{13}C_2$]-spermine ([1,1′-$^{13}C_2$]-*N*,*N*′-bis(3′-aminopropyl)-1,4-diamine) was synthesized from 1,4-diaminobutane (Fluka) and 3-^{13}C-acrylonitrile (Isotec) following the method of Israel et al. (1964). The molecular structure of [1,1′-$^{13}C_2$]-spermine and the labeling scheme is shown in Fig. 1a. The two symmetrical ^{13}C-labeled sites are designated with asterisks. The oligonucleotides were synthesized and HPLC-purified by Geneworks (Adelaide, Australia) and dialyzed extensively prior to use. All the complexes were 1 mM or less in DNA and had a stoichiometry as near as possible to 1:1 [1,1′-$^{13}C_2$]-spermine:DNA structure. All complexes were formed as described previously (Keniry 2003). Schematic diagrams of the structures formed by each of the oligonucleotides are shown in Fig. 1b.

NMR relaxation measurements

The NMR spectra were recorded at 25°C on Varian INOVA-300, 500 and 600 NMR spectrometers and a Bruker Avance-800 spectrometer (^{13}C frequencies of 75.4, 125.7, 150.9 and 201.2 MHz respectively). All samples were degassed and sealed in stoppered NMR tubes prior to measurement. ^{13}C spin-lattice relaxation measurements were determined using a cross-correlation suppressed T_1 method (Jin et al. 2003). The method is based on a proton-detected heteronuclear correlation experiment that uses a combination of radio-frequency pulses and pulsed field gradients to suppress dipole–dipole cross-correlated relaxation effects. ^{13}C spin–spin (transverse) relaxation rates were recorded using a indirect detection of the $\alpha_{2''}$ ^{13}C resonance with an experiment that had a variable ^{13}C CPMG delay (Farrow et al. 1994). Between nine and eleven delay periods were collected for each T_1 and T_2 experiment. Steady-state $\{^1H\}^{13}C$ NOEs were recorded with the standard gated decoupling technique using a recycle delay greater than $10\times T_1$. Spectra were recorded in the presence and absence of proton saturation, which was achieved with the use of 120° ^1H pulses applied every 5 ms for a total saturation time of 2 s. The errors in the relaxation times are expressed as one standard deviation, which was estimated from the quality of the two-parameter exponential fit of the data. Errors in the NOEs are estimates from the reproducibility of five independent experiments of some selected NOEs.

Data analysis

Motional parameters were determined from the relaxation rates and NOE enhancements following a Monte Carlo minimization procedure first described by Mayo and co-workers (Idiyatullin et al. 2003). Briefly, a Mathematica program was used to calculate spectral densities by minimizing the function

$$\chi^2 = \sum_i ([(R^i_{1\mathrm{exp}} - R^i_{1\mathrm{theor}})/\sigma_{R_1}]^2 + [(R^i_{2\mathrm{exp}} - R^i_{2\mathrm{theor}})/\sigma_{R_2}]^2 + [(\mathrm{NOE}^i_{\mathrm{exp}} - \mathrm{NOE}^i_{\mathrm{theor}})/\sigma_{\mathrm{NOE}}]^2) \quad (1)$$

where $R^i_{1\mathrm{exp}}$, $R^i_{2\mathrm{exp}}$, $\mathrm{NOE}^i_{\mathrm{exp}}$ are the experimental values and $R^i_{1\mathrm{theor}}$, $R^i_{2\mathrm{theor}}$, $\mathrm{NOE}^i_{\mathrm{theor}}$ are the calculated values of the NMR relaxation parameters and σ_{R_1} σ_{R_2}, σ_{NOE} are the estimated errors of the parameters. The relaxation parameters are expressed in terms of the spectral density functions.

$$R_1 = \frac{1}{10} B_{\mathrm{DD}} [J(\omega_{\mathrm{C}} - \omega_{\mathrm{H}}) + 3J(\omega_{\mathrm{C}}) + 6J(\omega_{\mathrm{C}} + \omega_{\mathrm{H}})] + \frac{2}{15} \Delta\sigma^2 \omega_{\mathrm{C}}^2 J(\omega_{\mathrm{C}}) \quad (2)$$

$$R_2 = \frac{1}{20}B_{DD}[J(\omega_C - \omega_H) + 3J(\omega_C) + 6J(\omega_C + \omega_H)] + 4J(0) + 6J(\omega_H)] + \frac{1}{45}\Delta\sigma^2\omega_C^2[4J(0) + 3J(\omega_C] + R_{ex} \quad (3)$$

$$NOE = \frac{1}{10}\frac{\gamma_H}{\gamma_C}\frac{[6J(\omega_C + \omega_H) - J(\omega_C - \omega_H)]}{R_1} \quad (4)$$

where $B_{DD} = n\gamma_C^2\gamma_H^2\hbar^2/r_{CH}^6 \cdot \gamma_H$ and γ_C are the magnetogyric ratios of the ^{1}H and ^{13}C nuclei, respectively, ħ is Plank's constant; r_{CH} is the length of the CH bond and n is the number of attached protons. $\Delta\sigma$, the chemical shift anisotropy for ^{13}C, is –25 ppm. The spectral density functions are themselves expressed in terms of the sum of five Lorentzians which is the maximum justified by the ten independent experimental parameters.

$$J(\omega) = \sum_{i=0}^{4}\frac{c_i\tau_i}{1 + \omega^2\tau_i^2} \quad (5)$$

where τ_i is the motional correlation times and c_i is the weighting coefficients. Equation (4) is not strictly correct for methylene carbons because of dipolar cross-correlation effects, but because of the substantial contribution from fast motions that are evident in the spermine dynamics, these cross-correlation contributions are not expected to influence the semi-quantitative comparison of spermine dynamics in this study.

The frequency dependent order parameter, $S^2(\omega)$ (Idiyatullin et al. 2003) is the squared order parameter for all motions with correlation time τ_i less than $1/\omega$ and is defined in terms of the weighting coefficients, c_i, such that

$$S^2(\omega_k) = 1 - \sum_{i=k}^{N} c_i \quad (6)$$

for all c_i whose associated correlation time satisfies the relation $\tau_i < 1/\omega$ (Idiyatullin et al. 2003). The Monte Carlo method for determining $S^2(\omega)$ followed the procedure outlined by Mayo and co-workers (Idiyatullin et al. 2003). The quality of the Monte Carlo simulations of the $S^2(\omega)$ curves was evaluated by back-calculation of the relaxation times and NOEs using the program, RELMODEL (version 301, Idityatullin et al. 2003), from τ_i and c_i extracted from the $S^2(\omega)$ curves. Two thirds of the relaxation times were within the errors quoted in Table 1 and the remaining values in Table 1 were within twice the error quoted in Table 1.

Results

^{13}C T_1relaxation times and heteronuclear NOEs

The spin–lattice, and spin–spin relaxation rate constants and NOE of the α_2'' carbon in [1,1′-$^{13}C_2$]-spermine either free in the unbound state or bound to duplex or quadruplex DNA are listed in Table 1. Sample R_1 and R_2 relaxation decay curves at a ^{13}C frequency of 150 MHz are presented in Fig. 2. The relaxation decays follow, to a good approximation, monoexponential decays. This shows that the pulse sequence used to measure the R_1 relaxation rate has suppressed the dipole–dipole cross-correlation effects from the methylene protons. Sample ^{13}C-edited spectra of the T_1 and T_2 measurements for spermine bound to the linear and folded quadruplexes are shown in

Table 1 Experimental values of ^{13}C proton decoupled relaxation rates and NOEs for the α_2 carbons of ^{13}C-spermine bound to duplex and quadruplex DNA at four different ^{13}C frequencies

Complex		75 MHz	125 MHz	150 MHz	200 MHz
Spermine	R_1 (s^{-1})	1.34 ± 0.13	1.27 ± 0.06	1.19 ± 0.03	1.14 ± 0.04
	R_2 (s^{-1})			1.56 ± 0.21	1.41 ± 0.20
	NOE	1.90 ± 0.19	1.64 ± 0.16	1.54 ± 0.15	1.58 ± 0.16
Spermine + 6 mer duplex	R_1 (s^{-1})	2.45 ± 0.14	2.02 ± 0.05	1.83 ± 0.07	1.75 ± 0.05
	R_2 (s^{-1})			3.42 ± 0.27	2.70 ± 0.38
	NOE	1.38 ± 0.14	1.45 ± 0.15	1.32 ± 0.13	1.30 ± 0.13
Spermine + 13 mer duplex	R_1 (s^{-1})	3.32 ± 0.20	2.63 ± 0.08	2.40 ± 0.08	2.24 ± 0.15
	R_2 (s^{-1})			4.46 ± 0.40	3.57 ± 0.45
	NOE	1.34 ± 0.13	1.30 ± 0.13	1.18 ± 0.12	1.14 ± 0.12
Spermine + linear quadruplex	R_1 (s^{-1})	3.03 ± 0.23	2.42 ± 0.19	2.30 ± 0.08	2.12 ± 0.07
	R_2 (s^{-1})			3.97 ± 0.33	3.28 ± 0.52
	NOE	1.48 ± 0.15	1.30 ± 0.13	1.29 ± 0.13	1.22 ± 0.13
Spermine + folded quadruplex	R_1 (s^{-1})	5.26 ± 0.46	3.82 ± 0.19	3.18 ± 0.21	2.63 ± 0.27
	R_2 (s^{-1})			16.1 ± 1.2	14.9 ± 1.8
	NOE	1.02 ± 0.10	0.99 ± 0.10	0.99 ± 0.10	0.99 ± 0.10

All data were recorded at 25 °C

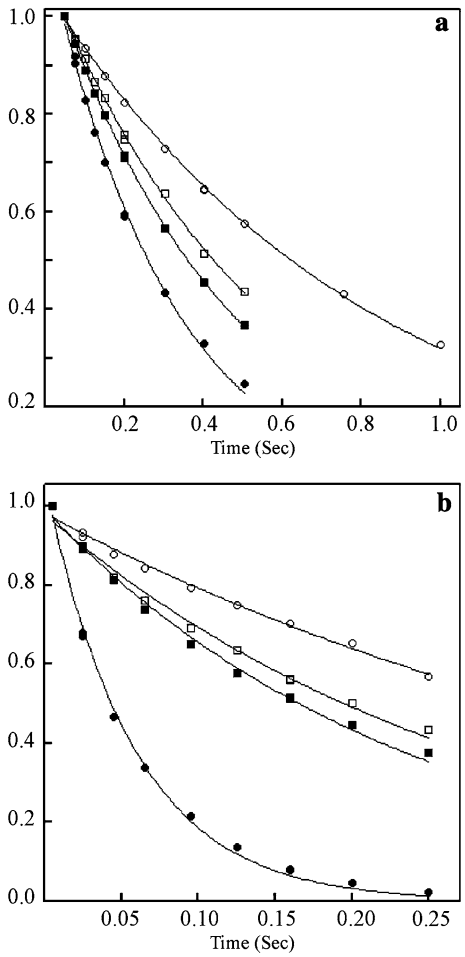

Fig. 2 Experimental T_1 (**a**) and T_2 (**b**) relaxation decay curves of the α_2'' $^{13}CH_2$ group of spermine at a carbon frequency of 150 MHz and at 25°C for the following solutions: 4 mM [1,1′-$^{13}C_2$]-spermine (*circle*), 1 mM [1,1′-$^{13}C_2$]-spermine-d(ATG-CAT)$_2$ (*square*), 1 mM [1,1′-$^{13}C_2$]-spermine-d(C_2TGTG$_2$ATA$_2$-CA).d(TGT$_2$ATC$_2$ACAG$_2$) (*filled square*), and 1 mM [1,1′-$^{13}C_2$]-spermine-d($G_4T_4G_4$)$_2$ (*filled circle*). All solutions were in 10 mM phosphate, 50 mM NaCl pH 7 D_2O buffer

Fig. S1 and the relaxation decay curves for the ^{13}C frequencies 200, 125 and 75 MHz are shown in Figs. S2, S3 and S4, respectively.

The R_1 and R_2 relaxation rates of free spermine are slow and the heteronuclear NOE is close to the theoretical maximum, which is characteristic of a rapidly tumbling small molecule with a substantial contribution from fast internal motion. The relaxation rates and the heteronuclear NOEs of spermine bound to either the hexamer, 13 mer or the linear quadruplex are surprisingly similar. The relaxation rates of all of the DNA-bound spermine are much slower than might be expected if the spermine was rigidly bound to the DNA, indicating that there is a substantial contribution to the relaxation from either motion of spermine on the DNA macromolecule or some internal motion of the $\alpha_{2''}$ methylene group that is characteristic of nucleotide-bound spermine. The relaxation rates of spermine bound to the folded quadruplex are faster than any of the other spermine-DNA complexes. The very fast R_2 rate suggests there is a substantial contribution from an exchange process that is occurring on the microsecond–millisecond timescale.

NMR relaxation data in proteins and DNA is frequently analyzed using the Lipari-Szabo model-free approach (Lipari and Szabo 1982) or a variation of this approach (Clore et al. 1990; Palmer et al. 1991). Model-free formalisms are preferable because the experimental data is usually insufficient to describe fully the complex motions of ligands that take place on the macromolecules. Motions of spermine bound to DNA are expected to be complex because it has been shown previously that there is substantial mobility that is independent of the overall tumbling of the DNA fragment even under conditions where most of the spermine is bound to the DNA (Wemmer et al. 1985; Banville et al. 1991; Keniry 2003). Although the effective correlation time of spermine bound to B-DNA has been estimated at less than 400 ps (Van Dam and Nordenskiöld 1999), there has been no in depth analysis of the motions and the correlation times that contribute to the independent motion of spermine on DNA. In order to address this deficit and to further explore the unusual character of spermine dynamics when bound to folded DNA quadruplexes, we have semi-quantitatively analyzed the dynamics of spermine using a variation of the model-free method. First introduced by Mayo and coworkers (Idiyatullin et al. 2003), this method uses a Monte Carlo approach to derive frequency-dependent order parameters, $S^2(\omega)$, that describe motions from the picosecond to nanosecond timescale. The frequency-dependent order parameter is defined as the squared order parameter for all motions with frequencies greater than ω (Idiyatullin et al. 2003). The method assumes that the spectral density function can be described by a sum of Lorentzians. In our analysis, we have assumed a maximum of five Lorentzians that is justified by the ten independent relaxation data measurements per sample.

An excellent description of the interpretation of the function, $S^2(\omega)$, is given by Idiyatullin et al. (2003) and we will briefly reproduce it here using a plot of $S^2(\omega)$ against $1/\omega$ for spermine bound to the folded quadruplex [d($G_4T_4G_4$)]$_2$, (Fig. 3) as an example. The data in Fig. 3 also show the extent of the errors in the curve, which are greatest at the inflection points (Idiyatullin et al. 2003). Large inflections occur at the correlation time of characteristic motions. Figure 3 shows there

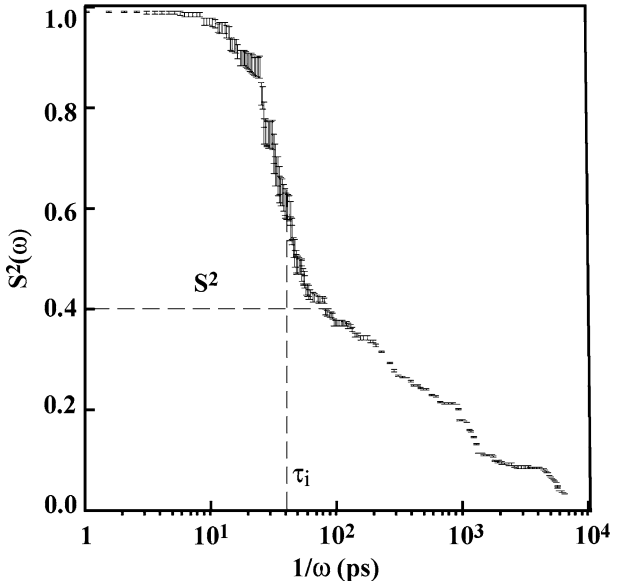

Fig. 3 Frequency-dependent order parameter function for the α_2'' $^{13}CH_2$ group in [1,1′-$^{13}C_2$]-spermine-d($G_4T_4G_4$)$_2$. $S^2(\omega)$ was calculated from ^{13}C T_1, T_2 and steady-state $\{^1H\}^{13}C$ NOE data acquired at four frequencies (75, 125, 150 and 200 MHz ^{13}C spectrometer frequencies) at 25°C. Spectral density functions were presumed to be a sum of five Lorenztians

are two main motional modes for spermine bound to the folded quadruplex illustrated by the two dominant inflections at ~50 ps and ~4 ns. The lowest frequency mode ($\tau_0 \approx 4$ ns) is due to the overall tumbling of the quadruplex indicating there is a binding site on [d($G_4T_4G_4$)]$_2$ that is sufficiently long lived to make a substantial contribution to the ^{13}C relaxation. There is a higher frequency ($\tau_i \approx 50$ ps) mode, which is due to restricted internal motion of spermine on the quadruplex. The generalized order parameter, S^2, which is the squared order parameter for all internal motions, can be read off the Y-axis and is defined by the height of the lower plateau (Fig. 3). The low frequency inflections are not sharp nor is the plateau that defines the generalized order parameter flat. This is most likely a limitation of the Monte Carlo method when analyzing real relaxation data from complicated motional regimes where a distribution of slow and partially restricted motions with closely related correlation times contribute to the relaxation. The plateau and inflection for the faster internal motion is better defined. This same trend is followed for the frequency-dependent order parameter curves for all spermine-DNA complexes. Hence, we will quote only the maximum value of S^2 for each of the spermine-DNA complexes. The generalized order parameter, S^2, provides an approximate measure of the dynamics of the α_2'' methylene of spermine. A value of $S^2 = 1$ implies that the α_2'' methylene is fixed relative to the frame of the DNA macromolecule and a value of $S^2 = 0$ implies that the α_2'' methylene is reorienting isotropically with respect to the overall tumbling of the DNA.

In Fig. 4 we compare the $S^2(\omega)$ function of unbound spermine and spermine bound to two different duplex DNA fragments. One is a self-complementary hexamer and the other is a complementary 13 mer. The relaxation parameters for spermine bound to these two duplexes are very similar and it is not surprising that they show similar $S^2(\omega)$ functions. The calculated $S^2(\omega)$ function for free spermine is shown for comparison but the model-free approach is least accurate in this case because the relaxation parameters even at the highest ^{13}C frequency (201 MHz) are least sensitive to the very fast motions in free spermine. This explains the gradual decline in slope from 1 to 5 ps. The sharp inflection at 30 ps is due to the overall tumbling of the spermine molecule. In contrast, the internal motion of spermine bound to the hexamer and the 13 mer dominates the relaxation. The high frequency inflection in the curve is sharp for spermine bound to both duplexes and occurs at correlation times of ~30 ps for the hexamer-bound spermine and ~50 ps for the 13-mer bound spermine. These correlation times are characteristic of fast restricted internal motion. There is no evidence for any contribution to the relaxation rates from unbound spermine and no exchange term, R_{ex}, was required to fit the data.

A previous study has shown that spermine is more immobile on folded DNA quadruplexes than a linear quadruplex, which has no loops (Keniry 2003). Figure 5 compares the $S^2(\omega)$ function for spermine bound to a linear quadruplex [d(TG_4T)]$_4$ and a folded quadruplex [d($G_4T_4G_4$)]$_2$. The $S^2(\omega)$ function for [d(TG_4T)]$_4$-bound spermine is remarkably similar to the curve for 13-mer bound spermine (Fig. 4) since both curves have a large contribution from internal motion with a correlation time of ~50 ps. In contrast [d($G_4T_4G_4$)]$_2$-bound spermine has a lesser contribution from the fast internal motion, which remarkably has the same characteristic correlation time of ~50 ps as the other DNA structures. The large generalized order parameter and the substantial contribution to the relaxation rates from the overall tumbling of the quadruplex verifies that there is a least one site on this quadruplex where spermine is relatively immobile. The model-free analysis of the relaxation data for [d($G_4T_4G_4$)]$_2$–bound spermine was the only one that required a non-zero value of R_{ex} (5.3 ± 1.0 s^{-1}) because of the contribution from the large R_2 values. This suggests that the relaxation of the α_2'' carbon resonance

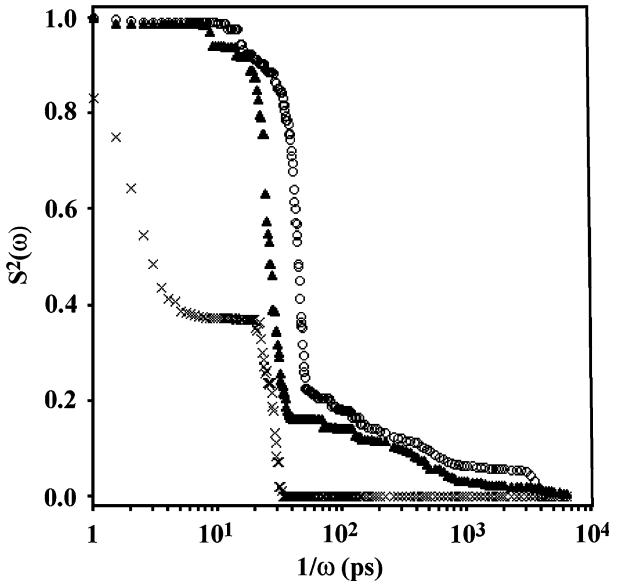

Fig. 4 Frequency-dependent order parameter function for the α_2'' $^{13}CH_2$ group in [1,1′-$^{13}C_2$]-spermine (*times*), [1,1′-$^{13}C_2$]-spermine-d(ATGCAT)$_2$ (*filled triangle*) and [1,1′-$^{13}C_2$]-spermine-d($C_2TGTG_2ATA_2CA$).d($TGT_2ATC_2ACAG_2$) (*circle*). $S^2(\omega)$ was calculated from ^{13}C T_1, T_2 and steady-state $\{^1H\}^{13}C$ NOE data acquired at four frequencies (75, 125, 150 and 200 MHz ^{13}C spectrometer frequencies) at 25°C. Spectral density functions were presumed to be a sum of five Lorenztians

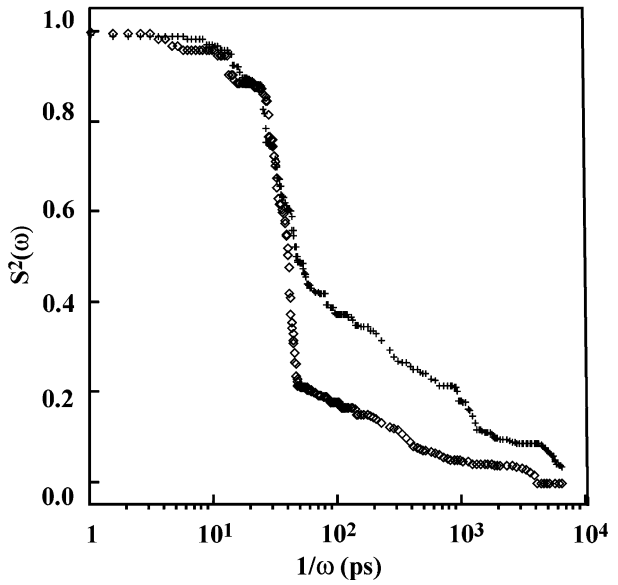

Fig. 5 Frequency-dependent order parameter function for the α_2'' $^{13}CH_2$ group in 1 mM [1,1′-$^{13}C_2$]-spermine-d(TG_4T)$_4$ (*diamond*) and 1 mM [1,1′-$^{13}C_2$]-spermine-d($G_4T_4G_4$)$_2$ (*plus*). $S^2(\omega)$ was calculated from ^{13}C T_1, T_2 and steady-state $\{^1H\}^{13}C$ NOE data acquired at four frequencies (75, 125, 150 and 200 MHz ^{13}C spectrometer frequencies) at 25°C. Spectral density functions were presumed to be a sum of five Lorenztians

of [d($G_4T_4G_4$)]$_2$-bound spermine is affected by a non-dipolar decay process. The most likely possibilities are a conformational exchange of the spermine methylene chain or a chemical exchange between two or more populations of bound spermine. The exchange must be rapid compared to the chemical shift difference of the populations because only one spermine resonance is observed in the temperature range of 5–30°C, although that resonance is broader than that of the bound spermine in any of the other spermine-DNA complexes. Since the calculated exchange rate depends on the chemical shift difference between the different populations of bound spermine, it is not possible to estimate the intrinsic exchange rate of even a simple two-site process except to say it must be in the millisecond–microsecond timescale.

Discussion

The polyamines are a family of molecules that exert their influence on cellular processes through weak interactions. They modulate gene expression (Thomas and Thomas 2001), protect DNA against radiation damage (Douki et al. 2000) and have apparently contradictory roles in protecting cells from apoptosis (Brüne et al. 1991) and facilitating cell death (Bello-Fernandez et al. 1993). Despite extensive study, the exact detail of how polyamines fulfill these roles has been elusive. There has been an ongoing search for some form of sequence specificity for polyamine binding but several X-ray (Drew et al. 1981), NMR (Van Dam and Nordenskiöld 1999; Wemmer et al. 1985; Banville et al. 1991) and theoretical studies (Korolev et al. 2001) have failed to provide convincing evidence for specific binding sites for polyamines on B-DNA. This is not surprising since the association of polyamines with DNA is dominated by the electrostatic interaction between the amines and the phosphates. There is growing evidence that the sequence specificity may arise from the structural flexibility of DNA. Polyamines have a greater affinity for certain structural elements in DNA such as the left-handed helix of Z-DNA (Van Dam and Nordenskiöld 1999; Banville et al. 1991; Thomas et al. 1991), the narrow groove of A-tracts (Lindemose et al. 2005), sequences that have a tendency to form A-DNA such as the estrogen receptor response element (Thomas et al. 1997; Lewis et al. 2000) and some folded quadruplex structures (Keniry 2003). These structural elements may be able to match the distance between the amines of certain polyamines to the distance between the phosphates better than B-DNA. The bound polyamine

structure does not necessarily have to be the low energy all-*trans* conformation of the free polyamine. For example, spermine adopted a fish-hook structure in a crystal-structure of a spermine-t-RNA complex (Quigley et al. 1978) and the intramolecular ^{1}H–^{1}H NOEs of spermine bound to a DNA quadruplex were inconsistent with the all-*trans* conformation in the bound conformation of spermine (Keniry 2003).

The impetus for this work was to gain a clearer picture of the dynamics of DNA-bound spermine and to further clarify the apparent preference of spermine for folded DNA quadruplexes. Previously, NMR studies had shown that spermine associated with B-DNA but it reoriented in a way that was independent of the overall tumbling of the macromolecule (Wemmer et al. 1985). The effective correlation time of this motion was faster than 400 ps but no other details of the motion could be extracted from the ^{1}H–^{1}H NOE data that was available. Subsequently, negative intramolecular ^{1}H–^{1}H NOEs were observed for the association of spermine with Z-DNA (Van Dam and Nordenskiöld 1999; Banville et al. 1991) and two folded DNA quadruplexes (Keniry 2003) suggesting a longer effective correlation time for spermine. No intermolecular NOEs were observed in either of these studies and hence there was no evidence for any specific tight binding site. This present work shows that the dynamics of the aminopropyl arm of spermine when bound to B-DNA or a linear parallel quadruplex is dominated by the fast internal motion of the methylene groups. The correlation time of the fast internal motion of the $\alpha_{2''}$ methylene group (~50 ps) is much longer than for free spermine (<10 ps) and is consistent with the timescale for large amplitude but restricted motion. The generalized order parameter is at most 0.2, which suggests there is only a small population of binding sites where the aminopropyl arm of spermine is tightly held. The dynamics of the aminopropyl arm of spermine bound to the folded quadruplex, $[d(G_4T_4G_4)]_2$, are discernibly different. The fast motion has the same correlation time (~50 ps) as the other spermine-DNA complexes but there is now evidence of a substantial population of binding sites in which the aminopropyl arm is effectively held rigid on the nanosecond timescale. The low frequency plateau is not flat, hence, it is difficult to assign a number to S^2 but it is at most 0.42. The fast R_2 relaxation rates and the model-free analysis indicate an exchange process but cannot distinguish between conformational exchange of the aminopropyl arm of spermine or chemical exchange between the tightly held spermine and a more mobile population that appears to be characteristic of most forms of DNA. So far it has not been possible to identify the binding site of the more tightly bound spermine. The two most likely sites are the very narrow groove of $[d(G_4T_4G_4)]_2$ or the loop structure of this folded quadruplex (Keniry 2003). The extensive internal motion and exchange processes clearly modulate the intermolecular ^{1}H–^{1}H NOEs to the point where they are unobservable and so they cannot be used to identify close distance contacts between spermine and $[d(G_4T_4G_4)]_2$. We previously showed that that some of the imino resonances from the loop thymines are broadened in the presence of spermine (Keniry 2003) suggesting that the loop structure is affected by spermine binding. The precise location of the binding site and the conformation of the spermine at this site remain elusive.

Spermine modulates gene expression in a number of ways. The effect may be direct whereby spermine forms a ternary complex with DNA and a transacting protein or indirect where spermine induces or stabilizes a conformation in DNA that is essential for gene expression (Thomas et al. 1997). This latter mechanism takes on great significance as evidence grows for a regulatory role for quadruplexes at the promotor sites of growth regulatory genes (Sun et al. 2005; Dexheimer et al. 2006). There is a need for further study of the influence of elevated spermine levels found in many cancer cells on the regulation of these important control points of cell proliferation pathways. Spermine may not only influence the formation and stabilization of these quadruplexes by direct binding but also by inducing macroscopic bending and curvature during DNA condensation and decondensation (Thomas and Thomas 2001). The association of spermine does not necessarily need to be strong to influence an equilibrium between an active and inactive DNA structure and it is worth noting that the energy barriers between divergent structures in some quadruplexes are not large (Keniry 2001; Shafer and Smirnov 2001).

We have shown for the first time that there is more than one population of bound spermine on some DNA quadruplex structures and that an exchange process is associated with the presence of a substantial population of immobile spermine. The NMR markers that are most sensitive to the presence of this newly identified population of bound spermine are the ^{13}C T_2 relaxation time and the spermine ^{1}H–^{1}H intramolecular NOEs (Keniry 2003). These two parameters may be useful in identifying similar populations of spermine in other biologically significant DNA structures such as Z-DNA, A-tracts and the estrogen receptor response element. Understanding the capacity of polyamines to recognize DNA structural elements will not only enhance our understanding of gene expression but

will have an impact on therapeutic applications where polyamine analogs show promise in facilitating the cellular uptake of antisense and antigene agents (Marsh et al. 2004).

Acknowledgments This work benefited from the use of NMR facilities at the Australian National University. The authors wish to thank Mr. Rob Longmore for the synthesis of the ^{13}C-spermine, Kylie Clayton for technical assistance, Dr. Michael John for advice on Mathematica programming and Professor Richard Shafer for critical reading of the manuscript.

References

Aboul-ela F, Murchie AIH, Lilley DMJ (1992) NMR study of parallel-stranded tetraplex formation by the hexadeoxynucleotide d(TG_4T). Nature 360:280–282

Andreasson B, Nordenskiöld L, Braunlin WH (1996) An NMR self-diffusion study of the interactions between spermidine and oligonucleotides. Biopolymers 38:505–513

Bancroft D, Williams LD, Rich A, Egli M (1994) The low-temperature crystal structure of the pure-spermine form of Z-DNA reveals binding of a spermine molecule in the minor groove. Biochemistry 33:1073–1086

Banville DL, Feuerstein BG, Shafer RH (1991) ^{1}H and ^{31}P nuclear magnetic resonance studies of spermine binding to the Z-DNA form of d($m^5CGm^5CGm^5CG)_2$: evidence for decreased spermine mobility. J Mol Biol 219:585–590

Bello-Fernandez C, Packham G, Cleveland JL (1993) The ornithine decarboxylase gene is a transcriptional target of c-*Myc*. Proc Natl Acad Sci USA 90:7804–7808

Berchtold CM, Tamez P, Kensler TW, Casero RA Jr (1998) Inhibition of cell growth in $CaCO_2$ cells by the polyamine analog N^1-N^{12}-bis(ethyl)spermine is preceded by a reduction in MYC oncoprotein levels. J Cell Physiol 174:380–386

Brüne B, Hartzell P, Nicotera P, Orrenius S (1991) Spermine prevents endonuclease activation and apoptosis in thymocytes. Exp Cell Res 195:323–329

Clore GM, Szabo A, Bax A, Kay LE, Driscoll PC, Gronenborn AM (1990) Deviations from the simple two-parameter model-free approach to the interpretation of nitrogen-15 nuclear magnetic relaxation of proteins. J Am Chem Soc 112:4989–4991

Dai JX, Chen D, Jones RA, Hurley LH, Yang DZ (2006) NMR solution structure of the major G-quadruplex structure formed in the human BCL2 promoter region. Nucleic Acids Res 34:5133–5144

Dexheimer TS, Sun D, Hurley LH (2006) Deconvoluting the structural and drug-recognition complexity of the G-quadruplex-forming region upstream of the bcl-2 P1 promoter. J Am Chem Soc 128:5404–5415

Douki T, Bretonniere Y, Cadet J (2000) Protection against radiation-induced degradation of DNA bases by polyamines. Radiat Res 153:29–35

Drew HR, Wing RM, Takano T, Broka C, Tanaka S, Itakura K, Dickerson RE (1981) Strucuture of a B-DNA dodecamer. Conformation and dynamics. Proc Natl Acad Sci USA 78:2179–2183

Egli M, Tereshko V, Teplova M, Minasov G, Joachimiak A, Sanishvili R, Weeks CM, Miller R, Maier MA, An H et al (1998) X-ray crystallographic analysis of the hydration of A- and B-form DNA at atomic resolution. Biopolymers 48:234–252

Farrow NA, Muhandiram R, Singer AU, Pascal SM, Kay CM, Gish G, Shoelson SE, Pawson T, Forman-Kay JD, Kay LE (1994) Backbone dynamics of a free and a phosphopeptide-complexed Src homology 2 domain studied by ^{15}N NMR relaxation. Biochemistry 33:5984–6003

Gray BN, Owen EA, Keniry MA (1994) The solution conformation of a trisdecanucleotide containing the consensus binding site of the dnaA initiation protein. Eur J Biochem 226:115–124

Hurley LH (2001) Secondary DNA structures as molecular targets for cancer therapeutics. Biochem Soc Trans 29:692–696

Idiyatullin D, Daragan VA, Mayo KH (2003) Protein dynamics using frequency-dependent order parameters from analysis of NMR relaxation data. J Magn Reson 161:118–125

Israel M, Rosenfield JS, Modest EJ (1964) Analogs of spermine and spermidine. I. Synthesis of polymethylenepolyamines by reduction of cyanoethylated α,ω-alkylenediamines. J Med Chem 7:710–716

Jain S, Zon G, Sundaralingan M (1989) Base only binding of spermine in the deep groove of the A-DNA octamer d(GTGTACAC). Biochemistry 28:2360–2364

Jin C, Prompers JJ, Brüschweiler R (2003) Cross-correlation suppressed T_1 and NOE experiments for protein side-chain $^{13}CH_2$ groups. J Biomol NMR 26:241–247

Keniry MA (2001) Quadruplex structures in nucleic acids. Biopolymers 56:123–146

Keniry MA (2003) A comparison of the association of spermine with duplex and quadruplex DNA by NMR. FEBS Lett 542:153–158

Korolev N, Lyubartsev AP, Nordenskiöld L, Laaksonen A (2001) Spermine: an ''invisible'' component in the crystals of B-DNA. A grand canonical Monte Carlo and molecular dynamics simulation study. J Mol Biol 308:907–917

Korolev N, Lyubartsev AP, Laaksonen A, Nordenskiöld L (2002) On the competition between water, sodium ions, and spermine in binding to DNA: a molecular dynamics computer simulation study. Biophys J 82:2860–2875

Lewis JS, Thomas TJ, Shirahata A, Thomas T (2000) Self-assembly of an oligodeoxyribonucleotide harboring the estrogen response element in the presence of polyamines: ionic, structural and DNA sequence specificity effects. Biomacromolecules 1:339–349

Lindemose S, Nielsen PF, Møllegaard NE (2005) Polyamines preferentially interact with bent adenine tracts in double-stranded DNA. Nucleic Acids Res 33:1790–1803

Lipari G, Szabo A (1982) Model-free approach to the interpretation of nuclear magnetic relaxation in macromolecules. 1. Theory and range of validity. J Am Chem Soc 104:4546–4559

Liquori AM, Constantino L, Crescenzi V, Elia V, Giglio E, Puliti R, De Santis Savino M, Vitagliano V (1967) Complexes between DNA and polyamines: a molecular model. J Mol Biol 24:113–122

Marsh AJ, Williams DM, Grasby JA (2004) The synthesis and properties of oligoribonucleotide-spermine conjugates. Org Biomol Chem 2:2103–2112

Marton LJ, Pegg AE (1995) Polyamines as targets for therapeutic intervention. Annu Rev Pharmacol Toxicol 35:55–91

Ohishi H, Terasoma N, Nakanishi I, van der Marel G, Van Boom JH, Rich A, Wang AHJ, Hakoshima T, Tomita K (1996) Interaction between left-handed Z-DNA and polyamine. 3. The crystal structure of the $d(CG)_3$ and thermospermine complex. FEBS Lett 398:291–296

Ouameur AA, Tajmir-Riahi H-A (2004) Strucutural analysis of DNA interactions with biogenic polyamines and

cobalt(III)hexamine studied by fourier transform infrared and capillary electrophoresis. J Biol Chem 279:42041–42054

Palmer III AG, Rance M, Wright PE (1991) Intramolecular motions of a zinc finger DNA-binding domain from Xfin characterized by proton-detected natural abundance ^{13}C heteronuclear spectroscopy. J Am Chem Soc 113:4371–4380

Phillips K, Dauter Z, Murchie AIH, Lilley DMJ, Luisi B (1997) The crystal structure of a parallel-stranded guanine tetraplex at 0.95Å resolution. J Mol Biol 273:171–182

Quigley GJ, Teeter MM, Rich A (1978) Structural analysis of spermine and magnesium-ion binding to yeast phenylalanine transfer-RNA. Proc Natl Acad Sci USA 75:64–68

Ruiz-Chica J, Medina MA, Sánchez-Jiménez F, Ramírez FJ (2001) Fourier transform Raman study of the structural specificities on the interaction between DNA and biogenic polyamines. Biophys J 80:443–454

Schmid N, Behr J-P (1991) Location of spermine and other polyamines on DNA as revealed by photoaffinity cleavage with poly(amino)benzenediazonium salts. Biochemistry 30:4357–4361

Shafer RH, Smirnov I (2001) Biological aspects of DNA/RNA quadruplexes. Biopolymers 56:209–227

Siddiqui-Jain A, Grand CL, Bearss DJ, Hurley LH (2002) Direct evidence for a G-quadruplex in a promotor region and its targeting with a small molecule to repress c-*Myc* transcription. Proc Natl Acad Sci USA 99:11593–11598

Smith FW, Feigon J (1992) Quadruplex structure of *Oxytricha* telomeric DNA oligonucleotides. Nature 356:164–168

Sun DY, Guo KX, Rusche JJ, Hurley LH (2005) Facilitation of a structural transition in the polypurine/polypyrimidine tract within the proximal promoter region of the human VEGF gene by the presence of potassium and G-quadruplex-interactive agents. Nucleic Acids Res 33:6070–6080

Tabor CW, Tabor H (1984) Polyamines. Annu Rev Biochem 53:749–790

Thomas T, Thomas TJ (1993) Selectivity of polyamines in triplex DNA stabilization. Biochemistry 32:14068–14074

Thomas T, Thomas TJ (2001) Polyamines in cell growth and cell death: Molecular mechanisms and therapeutic applications. Cell Mol Life Sci 58:244–258

Thomas TJ, Gunnia UB, Thomas T (1991) Polyamine-induced B-DNA to Z-DNA conformational transition of a plasmid DNA with (dG-dC)N insert. J Biol Chem 266:6137–6141

Thomas T, Kulkarni GD, Gallo MA, Greenfield N, Lewis JS, Shirahata A, Thomas TJ (1997) Effects of natural and synthetic polyamines on the conformation of an oligodeoxyribonucleotide with the estrogen response element. Nucleic Acids Res 25:2396–2402

Tippin DB, Sundaralingam M (1997) Nine polymorphic crystal structures of d(CCGGGCCCGG), d(CCGGGCCm^5CGG), d(Cm^5CGGGCCm^5CGG) and d(CCGGGCC(Br)^{5}CGG) in three different conformations: effects of spermine binding and methylation on the bending and condensation of *A*-DNA. J Mol Biol 267:1171–1185

Van Dam L, Nordenskiöld L (1999) Interactions of polyamines with the DNA octamers d($m^5CG)_4$ and d(GGAATTCC): a ^{1}H-NMR investigation. Biopolymers 49:41–53

Wang AH-J, Quigley GJ, Kolpak FJ, Crawford JL, Van Boom JH, Marel GVDM, Rich A (1979) Molecular structure of a left-handed double helical DNA fragment at atomic resolution. Nature 282:680–686

Wemmer DE, Srivenugopal KS, Reid BR, Morris DR (1985) Nuclear magnetic resonance studies of polyamine binding to a defined DNA sequence. J Mol Biol 185:457–459